Princeton Plasma Physics Laboratory

PPPL- 5028

PPPL- 5028

Inferring Magnetospheric Heavy Ion Density Using EMIC Waves

Eun-Hwa Kim, J.R. Johnson, H. Kim and Dong-Hun Lee

MAY, 2014

PRINCETON PLASMA PHYSICS LABORATORY

Prepared for the U.S. Department of Energy under Contract DE-AC02-09CH11466.

Inferring Magnetospheric Heavy Ion Density using EMIC waves

Eun-Hwa Kim[1], Jay R. Johnson[1], Hyomin Kim[2] and Dong-Hun Lee[3]

We present a method to infer heavy ion concentration ratios from EMIC wave observations that result from ion-ion hybrid (IIH) resonance. A key feature of the ion-ion hybrid resonance is the concentration of wave energy in a field-aligned resonant mode that exhibits linear polarization. This mode converted wave is localized at the location where the frequency of a compressional wave driver matches the IIH resonance condition, which depends sensitively on the heavy ion concentration. This dependence makes it possible to estimate the heavy ion concentration ratio. In this letter, we evaluate the absorption coefficients at the IIH resonance at Earth's geosynchronous orbit for variable concentrations of He^+ and field-aligned wave numbers using a dipole magnetic field. Although wave absorption occurs for a wide range of heavy ion concentrations, it only occurs for a limited range of field-aligned wave numbers such that the IIH resonance frequency is close to, but not exactly the same as the crossover frequency. Using the wave absorption and observed EMIC waves from GOES-12 satellite, we demonstrate how this technique can be used to estimate that the He^+ concentration is around 4% near $L = 6.6$.

1. Introduction

The presence of heavy ions can have a profound impact on the time response of the magnetosphere to internal and external forcing and can play a significant role in plasma entry and transport processes within the magnetosphere and ionosphere. Although satellites have directly detected heavy ion compositions and densities [e.g., *Chappell*, 1982; *Horwitz et al.*, 1984; *Farrugia et al.*, 1989; *Craven et al.*, 1997; *Bouhram et al.*, 2005], particle instruments have difficulty measuring cold plasma because of spacecraft charging effects and low flux of low velocity particles. Consequently, significant attention has been given to indirect methods that employ ULF wave observations, which are affected by the presence of heavy ions. Field-line resonance eigenfrequencies have been used to estimate magnetospheric plasma mass densities [e.g., *Denton et al.*, 2004; *Menk et al.*, 2004; *Takahashi et al.*, 2006; *Nosé et al.*, 2011]. Comparison of electron density (from plasma wave observations) with mass density inferred from field-line resonance eigenfrequency measurements indicate that the "mean mass" is significantly larger than the proton mass meaning that significant amount of heavy ions may be present [*Denton et al.*, 2004]. However, Alfvén resonant modes do not contain sufficient constraints to distinguish between relative concentrations of heavy ions. On the other hand, because ULF waves at higher frequency, such as electromagnetic ion cyclotron (EMIC) waves, are particularly sensitive to heavy ion concentrations they may be even more useful to constrain heavy ion abundances through indirect measurement [e.g., *Fraser et al.*, 2005; *Sakaguchi et al.*, 2013].

EMIC waves are low frequency waves typically in the Pc 1-2 (0.2-5Hz) frequency range that are excited below the proton gyrofrequency and are commonly observed in the plasmasphere and magnetosphere. The polarization of these waves has been generally reported to be left-hand (LH); however, right-hand (RH) or linear polarizations have also been reported [e.g., *Fraser and McPherron*, 1982; *Anderson et al.*, 1992; *Min et al.*, 2012] and their origin is not fully understood. Figure 1 shows an example of the EMIC waves detected by GOES-12 that exhibit dominant power in linear polarization. In this figure, EMIC wave activity in the H^+ band occurs from 04:00 to 04:50 UT with frequency ranging from ∼0.35 to 0.45 Hz, and the wave polarization ellipticity in the plane perpendicular to the local magnetic fields indicates that the waves are largely linearly polarized.

Such linearly polarized EMIC waves are interesting because the wave modes should be predominantly LH or RH except at the crossover frequency ($\omega_{\rm cr}$) [*Smith and Brice*, 1964] or at oblique propagation near the multi-ion hybrid resonances [e.g., *Lee et al.*, 2008]. Although linear polarization can result from refraction [*Rauch and Roux*, 1982; *Horne and Thorne*, 1993], absorption at high latitudes [*Horne and Thorne*, 1997] likely limits such polarizations to higher latitudes. *Denton et al.* [1996] suggested that the linear polarization may result from superposition of two waves, but the mechanism requires multiple waves and appropriate differences in phase. Alternatively, *Lee et al.* [2008] suggested that linearly polarized EMIC waves can be generated via mode conversion near the ion-ion hybrid (IIH) resonance location. When the frequency of incoming compressional waves matches the IIH resonance condition in an increasing (or decreasing) heavy ion concentration or inhomogeneous magnetic field strength (B_0), wave energy from incoming compressional waves concentrates and mode converts to EMIC waves. Wave simulations using multi-fluid code showed that the mode-converted EMIC waves at the IIH resonance are strongly guided by the ambient magnetic field ($\mathbf{B}_0$) and have linear polarization [*Kim et al.*, 2008, 2013].

Since the incoming compressional fast waves efficiently convert to the EMIC waves at the IIH resonance and the IIH resonance frequency is a function of the heavy ion concentration ratio $\eta_{\rm ion} = N_{\rm ion}/N_{\rm e}$, where $N_{\rm e(ion)}$ is an electron (ion) number density, B_0 and field-aligned wave number ($k_\parallel$) [*Kim et al.*, 2008], the sharply peaked dependence of mode conversion on $k_\parallel$ with observed B_0 makes it possible to estimate $\eta_{\rm ion}$ [e.g., *Kazakov and Fülöp*, 2013] from the detected EMIC waves. Following this line of reasoning, in this letter we evaluate the general dependence of mode conversion on $k_\parallel$ and show how to infer the heavy ion density using observed EMIC waves. Previously, *Lee et al.* [2008] and *Kim et al.* [2011] had provided estimates of absorption at the IIH resonance for a given $k_\parallel$, but they did not provide the general dependence of absorption in $k_\parallel$, so we first generalize this work.

[1]Princeton Plasma Physics Laboratory, Princeton University, Princeton, New Jersey, USA.
[2]Center for Space Science and Engineering Research, Bradley Department of Electrical and Computer Engineering Virginia Tech, Virginia, USA.
[3]School of Space Research and Department of Astronomy and Space Science, Kyung Hee University, Yongin, Gyeonggi, Korea.

0094-8276/14/$5.00

2. Model Description

We estimate the efficiency of mode conversion of a radially propagating compressional wave at the IIH resonance using a simplified 1D slab cold plasma model that captures the essential features of the IIH resonance [*Kim et al.*, 2011]. The slab model is a local approximation where x, y, and z correspond to radial, azimuthal, and field-aligned coordinates. Wave propagation in the cold, fluid model can be described by Maxwell's equations combined with fluid equations for ions and electrons (ignoring electron inertial effects and background gradients related to diamagnetic drift and density compressions) [*Kim et al.*, 2011],

$$\frac{c}{\omega}\frac{\partial \mathbf{Y}}{\partial x} = \mathbf{MY}, \tag{1}$$

where

$$\mathbf{Y} = \begin{pmatrix} E_y \\ \frac{c}{\omega}\frac{\partial E_y}{\partial x} - i n_y E_x \end{pmatrix}, \tag{2}$$

and

$$\mathbf{M} = \begin{pmatrix} \frac{n_y \epsilon_d}{n_z^2 - \epsilon_s} & 1 + \frac{n_y^2}{n_z^2 - \epsilon_s} \\ \frac{(n_z^2 - \epsilon_r)(n_z^2 - \epsilon_l)}{n_z^2 - \epsilon_s} & -\frac{n_y \epsilon_d}{n_z^2 - \epsilon_s} \end{pmatrix}, \tag{3}$$

where n_y is the refractive index in the azimuthal direction and ϵ_r, ϵ_l, ϵ_d, and ϵ_s are the plasma electric tensor components in the notation of Stix [*Stix*, 1992]. Eqs. (1)-(3) have been solved with a finite difference approach with nonuniform mesh [e.g., *Johnson et al.*, 1995; *Johnson and Cheng*, 1999; *Kim et al.*, 2011]. Eq. (3) exhibits a singularity where

$$n_z^2 = \epsilon_s, \tag{4}$$

which is called the IIH resonance because it occurs between the two ion cyclotron frequencies. For $k_\parallel \to 0$, $\omega_{\rm ii}$ reduces to the Buchsbaum resonance frequency ($\omega_{\rm bb}$), which satisfies $\epsilon_s = 0$.

We solve Eq. (1) in terms of the normalized spatial variable, $L \equiv x/{\rm R_E}$, where ${\rm R_E}$ is the Earth's radii, and the inner and outer boundaries such that $6.1 \le L \le 7.1$ and assume the resonance occurs near Earth's geosynchronous orbit at $L = 6.6$. We adopt an electron-hydrogen-helium plasma in our model with a constant $\eta_{\rm He}$ in x. The B_0 and $N_{\rm e}$ at the magnetic equator are assumed to be [*Lee and Lysak*, 1989]

$$B_0 = \frac{B_s}{L^3}, \tag{5}$$

$$N_{\rm e} = N_{\rm mp}\frac{L_{\rm mp}^3}{L^3}, \tag{6}$$

where $B_s = 3.1 \times 10^{-5}$ T is magnetic field strength at the Earth's surface and $N_{\rm mp} = 10{\rm cm}^{-3}$ is the total density of the magnetopause at $L_{\rm mp} = 10$. Incoming waves are launched at the lower magnetic field region (i.e., outer magnetosphere) and the wave solution is decomposed into WKB solutions to determine reflection, transmission, and absorption coefficients at the boundaries.

3. Dispersion Relation

The refractive index perpendicular to $\mathbf{B}_0$ of incoming compressional waves can be derived as

$$n_\perp^2 \cong \frac{(\epsilon_r - n_z^2)(\epsilon_l - n_z^2)}{(\epsilon_s - n_z^2)}, \tag{7}$$

where subscription of $\perp$ represents the perpendicular $\mathbf{B}_0$, thus $n_\perp^2 = n_x^2 + n_y^2$. The $k_\perp = n_\perp \omega/c$ of incoming compressional waves along L are calculated as a function of $k_\parallel$ for $\eta_{\rm He} = 10\%$ as shown in Figure 2, where the resonance occurs at $L = 6.6$. Here, wavenumbers are normalized to $k_{\rm cr} = k_\parallel(\omega_{\rm ii} = \omega_{\rm cr})$, $K_{\perp(\parallel)} = k_{\perp(\parallel)}/k_{\rm cr}$, and K_y is assumed to be 0. Under the given plasma conditions, $\lambda_{\rm cr} = 2\pi/k_{\rm cr}$ is 0.107 ${\rm R_E}$ at $L = 6.6$.

In Figure 2, blank areas represent wave stop gaps where $K_\perp^2 < 0$. The boundaries of the wave stop gap are the resonance at $L = 6.6$ and cutoffs where $K_\perp^2 = 0$. At the inner boundary at $L = 6.1$, RH cutoff occurs ($K_\perp \to 0$) for $K_\parallel(K_{\perp,L=6.1}) \to 0) \sim 0.87$ and the compressional waves have a cutoff-resonance-cutoff triplet in x for $K_\parallel > K_\parallel(K_{\perp,L=6.1})$ and cutoff-resonance pair for $K_\parallel < K_\parallel(K_{\perp,L=6.1})$. When waves have a cutoff-resonance-cutoff triplet, absorption at the IIH resonance can occur both as the wave leaks through the resonance as well as when the wave reflects off the inner cutoff and propagates back into the resonance so that the wave absorption can be as large as 100% [e.g., *Kim et al.*, 2011], which is a characteristic of cutoff-resonance-cutoff conditions [*Karney et al.*, 1979; *Ram et al.*, 1996; *Lin et al.*, 2010].

Using plasma conditions at $L = 6.6$ ($B_0 = 108$nT and $N_{\rm e} = 34.7{\rm cm}^{-3}$), we calculate the IIH resonance frequency, $\Omega_{\rm ii} = \omega_{\rm ii}/\omega_{{\rm ci}(L=6.6)}$, where $\omega_{{\rm ci}(L=6.6)}$ is proton cyclotron frequency at $L = 6.6$, as a function of $\eta_{\rm He}$ and $K_\parallel$ in Figure 3a. This figure clearly shows that $\Omega_{\rm ii}$ increases when $\eta_{\rm He}$ and/or $K_\parallel$ increase. The value of $\Omega_{\rm ii}$ has a significant dependence on $K_\parallel$ ranging from $\Omega_{\rm ii} \approx \Omega_{\rm bb}$ for $K_\parallel \to 0$ to $\Omega_{\rm ii} \approx \Omega_{\rm cr}$ as $K_\parallel \to 1$.

Because $\Omega_{\rm ii}$ is a function of $\eta_{\rm He}$ and $K_\parallel$, $K_\parallel$ can also be expressed as a function of $\eta_{\rm He}$ and $\Omega_{\rm ii}$ as shown in Figure 3b. The value of $\Omega_{\rm ii}$ increases monochromatically with $\eta_{\rm He}$ and can be used to estimate $\eta_{\rm He}$ from Figure 3b, if strong wave absorption occurs. For example, when the linearly polarized EMIC waves are observed with $\Omega_{\rm obs} \approx \Omega_{\rm ii} = 0.6$ and if the maximum absorption is calculated at $K_\parallel^{\rm max} = 0.7$, $\eta_{\rm He}$ can be estimated as $\eta_{\rm He} \approx 44\%$. In Section 4, we calculate the wave absorption coefficient ($\mathcal{A}$) as a function of $K_\parallel$ and $\eta_{\rm He}$ and then $\mathcal{A}(K_\parallel, \eta_{\rm He})$. These results are then converted into $\mathcal{A}(\Omega_{\rm ii}, \eta_{\rm He})$ similar to Figure 3.

4. Wave Absorption at the IIH resonance

In Figure 4a, we calculate the absorption coefficient ($\mathcal{A}$) of the compressional waves as a function of $K_\parallel$ and $\eta_{\rm He}$ for no azimuthal wave number ($K_y = 0$). The maximum value of $\mathcal{A}$ ($\mathcal{A}^{\rm max}$) can be as large as 100% where $K_\parallel > K_\parallel(K_{\perp,L=6.1} \to 0)$. In this region, the waves encounter a cutoff-resonance-cutoff triplet, and thus $\mathcal{A}$ oscillates in both $K_\parallel$ and $\eta_{\rm He}$ due to the interference effect between incoming and reflected compressional waves. For $K_\parallel < K_\parallel(K_{\perp,L=6.1} \to 0)$, $\mathcal{A}^{\rm max}$ is near 25% which is the Budden limit of the cutoff-resonance pair. In Figure 4a, for $K_\parallel = 1$ at $\Omega_{\rm ii} = \Omega_{\rm cr}$, no absorption occurs, which is consistent with previous calculations [*Klimushkin et al.*, 2006; *Kim et al.*, 2011].

The edge of ΔK is clearly visible as a function of $\eta_{\rm He}$ in Figure 4a. For $\eta_{\rm He} \sim 1$ or 0, the absorption occurs in a relatively wide range of $K_\parallel$, however, for moderate $\eta_{\rm He}$, most absorption occurs for $0.9 \le K_\parallel \le 1$. This range of $K_\parallel$ is much higher and narrower than the range seen at Mercury where maximum efficiency occurs broadly for $K_\parallel = 0.5-0.8$ [*Kim et al.*, 2011; *Kim and Johnson*, 2014].

We convert $\mathcal{A}(K_\parallel, \eta_{\rm He})$ to $\mathcal{A}(\Omega_{\rm ii}, \eta_{\rm He})$ as shown in Figure 4b in order to show the frequency range where strong absorption occurs. The figure clearly shows that most absorption occurs near $\Omega_{\rm cr}$, where $K_\parallel \approx 1$, with narrow $\Delta\Omega$ and $\Delta\eta_{\rm He}$ (the maximum $\Delta\Omega$ and $\Delta\eta_{\rm He}$ are ~2.7% and 2.5%, respectively). In Figure 4b, we infer the He^+ concentration ratio from the observed EMIC waves in Figure 1. Wave frequencies at 4:15, 4:20, 4:25, and 4:30 UT are selected and the maximum and minimum frequencies at each time are (UT, $\Omega_{\rm obs}^{\rm min}$, $\Omega_{\rm obs}^{\rm max}$) $\approx$ (4:15, 0.29, 0.3), (4:20, 0.29, 0.34), (4:25, 0.27, 0.35), and (4:30, 0.28, 0.32). We plot the frequency ranges as a horizontal bars and the average values ($\overline{\Omega}_{\rm obs}$) between $\Omega_{\rm obs}^{\rm min}$ and $\Omega_{\rm obs}^{\rm max}$ as circles. Using the average frequencies, the $\eta_{\rm He}$ can be inferred to 3.3, 3.4, 4.2, and 3.6 $\pm$ 0.7%, respectively. Here, the minimum density ratio can be estimated by assuming that the average frequency is the crossover frequency ($\overline{\Omega}_{\rm obs} \approx \Omega_{\rm cr}$) and the maximum of $\eta_{\rm He}$ is $\sim$ 5%. Similarly, *Fraser et al.* [2005] estimated $\eta_{\rm He}$ to range between 6–16% inferred from GOES-8 and 10 observations of LH polarized EMIC waves.

5. Discussion and Summary

In this letter, we present a method to infer the heavy ion concentration ratio using observed EMIC waves at Earth's magnetosphere. At geosynchronous orbit near $L = 6.6$, we show that compressional wave absorption (the linearly polarized EMIC wave generation) occurs over a wide range of heavy ion concentration, while it occurs in a limited range of field-aligned wave numbers ($0.9 \le K_\parallel \le 1.0$). In these ranges of $K_\parallel$, the wavelength parallel to $\mathbf{B}_0$ is much shorter than one Earth radius ($0.04\mathrm{R_E} \le \lambda_\parallel \le 0.18\mathrm{R_E}$) and the IIH resonance frequency is close to the crossover frequency ($\Omega_{\rm ii} \approx \Omega_{\rm cr}$). Thus the heavy ion concentration ratio can be estimated using $\Omega_{\rm cr}$. Interestingly, this result was predicted by *Kazakov and Fülöp* [2013], although their approach does not provide an accurate estimate of wave absorption [*Kim and Johnson*, 2014] because it does not properly describe the cutoff-resonance-cutoff triplet.

This method should be useful for estimating the global structure of magnetospheric heavy ion concentrations from detected linearly polarized EMIC waves as shown in Figures 4. However, because the wave absorption is very sensitive to plasma conditions, such as density scale length, heavy ion density ratio, and magnetic field gradient, wave absorption for different magnetospheric environment should be considered. For example at Mercury, the value of $K_\parallel$ and the frequency ratio to the crossover frequency with maximum absorption are $0.5 \le K_\parallel \le 0.8$ and $0.5 \le \Omega_{\rm ii}/\Omega_{\rm cr} \le 0.9$ [*Kim et al.*, 2011; *Kim and Johnson*, 2014] rather than $\Omega_{\rm ii} \approx \Omega_{\rm cr}$ suggested by *Kazakov and Fülöp* [2013].

Moreover, the Buchsbaum resonance and the crossover frequencies can be used to constrain the upper and lower limits of the heavy ion concentration as the resonance condition will always occur between these two frequencies. *Lee et al.* [2008] suggested that when the incoming waves propagate from the inner magnetosphere and the field-aligned wavelength is larger than $0.7\mathrm{R_E}$ near the geosynchronous orbit, the mode conversion at the IIH resonance can occur near, but not the frequency same as the Buchsbaum resonance. In this case, $\eta_{\rm ion}$ can be estimated from $\omega_{\rm bb}$.

Although we demonstrated how ion density can be inferred from EMIC observations, there are several limitations in our calculations. The azimuthal wavenumber (K_y) is one of the important factors that controls absorption, but we only showed the wave absorption for $K_y = 0$. However, absorption tends to peak at smaller K_y, so the results shown should be reasonable. We have also calculated the wave absorption coefficient for $K_y = 0-0.3$ (not shown here) and found that the $K_\parallel$ window for wave absorption decreases when K_y increases and is less affected by K_y. Therefore, the results shown in Figure 4b are relevant for various K_y cases because we are interested in the range of $K_\parallel$ values for mode conversion.

Our analysis also assumed a constant heavy ion density concentration, although wave absorption can also occur

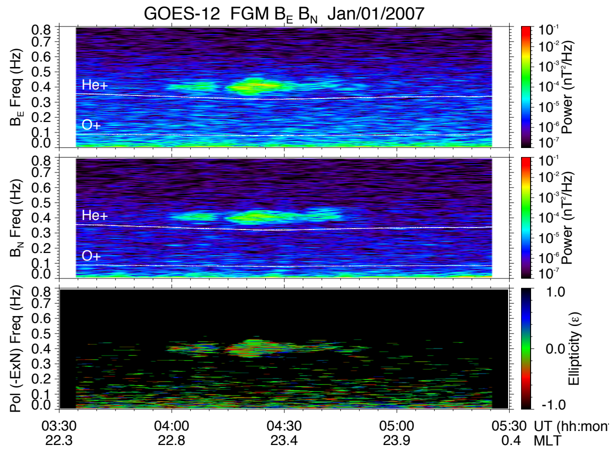

Figure 1. High-time resolution (512ms) Level 2 GOES-12 magnetic field data show EMIC wave activity in the H^+ band from 04:00 to 04:50 UT over the frequencies of $\sim$ 0.35 to 0.45 Hz. The top and middle panels present wave power as a function of frequency in the E and N components of the data, respectively. The GOES satellite magnetometers conform to the PEN coordinate system, in which B_P is a magnetic field vector component pointing northward, perpendicular to the orbit plane (parallel to Earths spin axis) and B_E points earthward, being perpendicular to B_P. B_N completes the Cartesian coordinate and points eastward. Wave polarization ellipticity in the plane perpendicular to the local magnetic fields (E and N) is shown in the bottom panel, indicating that the wave is largely linearly polarized.

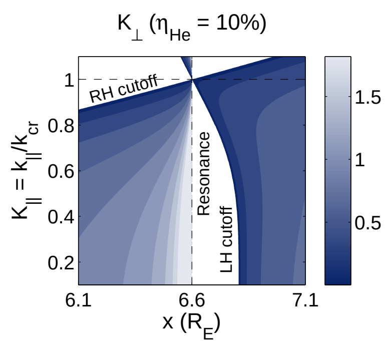

Figure 2. The refractive index $K_\perp = k_\perp/k_{\rm cr}$ of incoming compressional waves as a function of $K_\parallel = k_\parallel/k_{\rm cr}$ assuming the IIH resonance occurs at $L = 6.6$ for $\eta_{\rm He} = 10\%$. Here the horizontal and vertical axes are L and $K_\parallel$. Black solid and dashed lines are cutoffs and resonance conditions, respectively.

when plasma contains inhomogeneous heavy ion concentrations. Inhomogeneous heavy ion concentrations in the radial direction can also modify the radial structure of the IIH resonance frequency as well as the wave dispersion relation in space [*Kim et al.*, 2011]. The IIH resonance occurs between each pair of ion gyrofrequencies [e.g., *Kim et al.*, 2013], and inclusion of heavier ions, such as O^+, can possibly modify the $K_\parallel$ window for wave absorption. Therefore, detailed investigations of the effect of inhomogeneous heavy ion density in dipole magnetic field and comparative studies in different magnetospheres remains as future work.

In summary, we present a method to infer heavy ion concentrations using detected EMIC waves from satellites. Because linearly polarized EMIC waves can generated via mode conversion from the compressional waves depending on $k_\parallel$, peaked dependence of compressional wave absorption (thus generation of linearly polarized EMIC waves) enables us to estimate the heavy ion concentration ratio. We demonstrated that the maximum absorption occurs when the IIH resonance frequency is close to the crossover frequency at geosynchronous orbit and inferred heavy ion densities around $\sim 4\%$ from the observed waves from GOES-12 data.

Acknowledgments. The authors thank Prof. Mark Engebretson for his valuable comments. The work at the Princeton University was supported by NASA grants (NNH09AM53I, NNH09AK63I, NNH11AQ46I, and NNH13AV37I), NSF grants (ATM0902730 and AGS-1203299), and DOE contract DE-AC02-09CH11466. The work at Virginia Tech was supported by NSF grant PLR-1243398. The work at the Kyung Hee University was also supported by the BK21 Plus Program through the National Research Foundation of Korea, funded by the Ministry of Education, Science and Technology. The GOES spacecraft data were provided by the NOAA Space Weather Prediction Center.

References

Anderson, B. J., R. E. Erlandson, and L. J. Zanetti (1992), A statistical study of Pc 1-2 magnetic pulsations in the equatorial magnetosphere 1. Equatorial occurrence distributions, *J. Geophys. Res.*, *97*, 3075–3088.

Bouhram, M., et al. (2005), Survey of energetic O^+ ions near the dayside mid-latitude magnetopause with Cluster, *Ann. Geophys.*, *23*, 1281–1294, doi:10.5194/angeo-23-1281-2005.

Chappell, C. R. (1982), Initial observations of thermal plasma composition and energetics from Dynamics Explorer-1, *Geophys. Res. Lett.*, *9*, 929–932, doi:10.1029/GL009i009p00929.

Craven, P. D., D. L. Gallagher, and R. H. Comfort (1997), Relative concentration of He^+ in the inner magnetosphere as observed by the DE 1 retarding ion mass spectrometer, *J. Geophys. Res.*, *102*, 2279–2290, doi:10.1029/96JA02176.

Denton, R. E., B. J. Anderson, G. Ho, and D. C. Hamilton (1996), Effects of wave superposition on the polarization of electromagnetic ion cyclotron waves, *J. Geophys. Res.*, *101*, 24,869–24,886.

Denton, R. E., J. D. Menietti, J. Goldstein, S. L. Young, and R. R. Anderson (2004), Electron density in the magnetosphere, *J. Geophys. Res.*, *109*, 09,215.

Farrugia, C. J., J. Geiss, H. Balsiger, and D. T. Young (1989), The composition, temperature, and density structure of cold ions in the quiet terrestrial plasmasphere - GEOS 1 results, *J. Geophys. Res.*, *94*, 11,865–11,891, doi:10.1029/JA094iA09p11865.

Fraser, B. J., and R. L. McPherron (1982), Pc 1-2 magnetic pulsation spectra and heavy ion effects at synchronous orbit - ATS 6 results, *J. Geophys. Res.*, *87*, 4560–4566.

Fraser, B. J., H. J. Singer, M. L. Andrian, D. L. Gallagher, and M. F. Thomsen (2005), The Relationship between Plasma Density Structure and Emic Waves at Geosynchronous Orbit, in *Inner Magnetosphere Interactions: New Perspectives from Imaging*, edited by J. Burch, M. Schulz, and H. Spence, American Geophysical Union, Washington, D. C, doi:10.1029/159GM04.

Horne, R. B., and R. M. Thorne (1993), On the preferred source location for the convective amplification of ion cyclotron waves, *J. Geophy. Res.*, *98*, 9233, doi:10.1029/92JA02,972.

Horne, R. B., and R. M. Thorne (1997), Wave heating of He^+ by electromagnetic ion cyclotron waves in the magnetosphere: Heating near the H^+ – He^+ bi-ion resonance frequency, *J. Geophys. Res.*, *102*, 11,457.

Horwitz, J. L., R. H. Comfort, and C. R. Chappell (1984), Thermal ion composition measurements of the formation of the new outer plasmasphere and double plasmapause during storm recovery phase, *Geophys. Res. Lett.*, *11*, 701–704.

Johnson, J. R., and C. Z. Cheng (1999), Can ion cyclotron waves propagate to the ground?, *Geophys. Res. Lett.*, *26*, 671–674.

Johnson, J. R., T. Chang, and G. B. Crew (1995), A study of mode conversion in an oxygen-hydrogen plasma, *Phys. Plasmas*, *2*, 1274–1284.

Karney, C. F. F., F. W. Perkins, and S. Y. C. (1979), Alfven resonance Effects on Magnetosonic Modes in Large Tokamaks, *Phys. Rev. Lett.*, *24*, 1621.

Kazakov, Y. O., and T. Fülöp (2013), Mode conversion of waves in the Ion-cyclotron frequency range in magnetospheric plasmas, *Phys. Rev. Lett.*, *111*, 125,002, doi:10.1103/PhysRevLett.111.125002.

Kim, E.-H., and J. R. Johnson (2014), Comment on "Mode conversion of waves in the Ion-cyclotron frequency range in magnetospheric plasmas", accepted to *Phys. Rev. Lett.*

Kim, E. H., J. R. Johnson, and D. H. Lee (2008), Resonant absorption of ULF waves at Mercury's magnetosphere, *J. Geophys. Res.*, *113*, A11,207.

Kim, E.-H., J. R. Johnson, and K.-D. Lee (2011), ULF wave absorption at Mercury, *Geophys. Res. Lett.*, *38*, L16,111, doi:10.1029/2011GL048,621.

Kim, E.-H., J. R. Johnson, D.-H. Lee, and Y. S. Pyo (2013), Field-line resonance structure in Mercury's multi-ion magnetosphere, *Earth, Planets, and Space*, *65*, 447.

Klimushkin, D. Y., P. N. Mager, and K.-H. Glassmeier (2006), Axisymmetric Alfvén resonances in a multi-component plasma at finite ion gyrofrequency, *Ann. Geophys.*, *24*, 1077–1084.

Lee, D.-H., and R. L. Lysak (1989), Magnetospheric ULF wave coupling in the dipole model - The impulsive excitation, *J. Geophys. Res.*, *94*, 17,097–17,103.

Lee, D.-H., J. R. Johnson, K. Kim, and K.-S. Kim (2008), Effects of heavy ions on ULF wave resonances near the equatorial region, *J. Geophys. Res.*, *113*, A11,212, doi:10.1029/2008JA013,088.

Lin, Y., J. R. Johnson, and X. Y. Wang (2010), Hybrid simulation of mode conversion at the magnetopause, *J. Geophys. Res.*, *115*, A04,208, doi:doi:10.1029/2009JA014524.

Menk, F. W., I. R. Mann, A. J. Smith, C. L. Waters, M. A. Clilverd, and D. K. Milling (2004), Monitoring the plasmapause using geomagnetic field line resonances, *J. Geophys. Res.*, *109*, A04216, doi:10.1029/2003JA010097.

Min, K., J. Lee, K. Keika, and W. Li (2012), Global distribution of EMIC waves derived from THEMIS observations, *J. Geophys. Res.*, *117*, A05,219, doi:10.1029/2012JA017,515.

Nosé, M., K. Takahashi, R. R. Anderson, and H. J. Singer (2011), Oxygen torus in the deep inner magnetosphere and its contribution to recurrent process of O^+-rich ring current formation, *J. Geophys. Res.*, *116*, A10224, doi:10.1029/2011JA016651.

Ram, A. K., A. Bers, and S. D. Schultz (1996), Mode conversion of fast Alfvén waves at the ion-ion hybrid resonance, *Phys. Plasmas*, *3*, 1828.

Rauch, J. L., and A. Roux (1982), Ray tracing of ULF waves in a multicomponent magnetospheric plasma - Consequences for the generation mechanism of ion cyclotron waves, *J. Geophys. Res.*, *87*, 8191–8198.

Sakaguchi, K., Y. Kasahara, M. Shoji, Y. Omura, Y. Miyoshi, T. Nagatsuma, A. Kumamoto, and A. Matsuoka (2013), Akebono observations of EMIC waves in the slot region of the radiation belts, *Geophy. Res. Lett.*, *40*, 5587–5591, doi:10.1002/2013GL058258.

Smith, R. L., and N. Brice (1964), Propagation in multicomponent plasmas, *J. Geophys. Res.*, *69*, 5029–5040, doi:10.1029/JZ069i023p05029.

Stix, T. H. (1992), *Waves in plasmas*, American Institute of Physics, New York,.
Takahashi, K., R. E. Denton, R. R. Anderson, and W. J. Hughes (2006), Mass density inferred from toroidal wave frequencies and its comparison to electron density, *J. Geophys. Res.*, *111*, A01201, doi:10.1029/2005JA011286.

Corresponding author: E.-H. Kim, Plasma Physics Laboratory, Princeton University, Princeton, NJ 08543-0451, USA. (ehkim@pppl.gov)

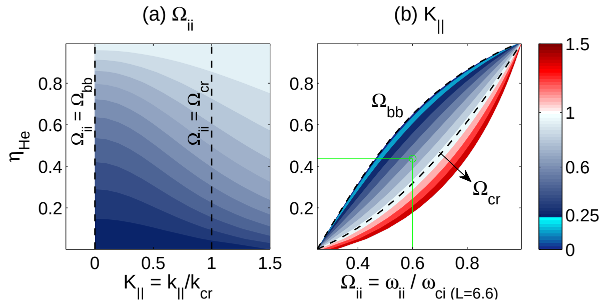

Figure 3. The normalized ion-ion hybrid resonance ($\Omega_{\rm ii} = \omega_{\rm ii}/\omega_{\rm ci}$) at $L = 6.6$ as a function of (a) $K_\|$ and $\eta_{\rm He}$ and (b) $\Omega_{\rm ii}$ and $\eta_{\rm He}$. Dashed lines represent the Buchsbaum resonance ($\Omega_{\rm bb}$) or the crossover frequency ($\Omega_{\rm cr}$). The heavy ion density ratio can be estimated using this figure. For example, when the linearly polarized EMIC waves are observed with $\Omega_{\rm obs} \approx \Omega_{\rm ii} = 0.6$ and the maximum absorption is calculated at $K_\|^{\rm max} = 0.7$, $\eta_{\rm He}$ can be estimated as $\eta_{\rm He} \approx 44\%$ (see green lines).

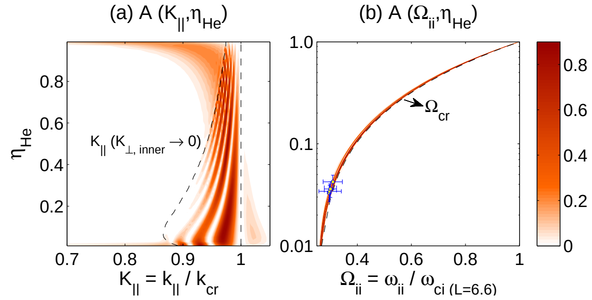

Figure 4. (a) The absorption coefficient ($\mathcal{A}$) for $K_y = 0$ as a function of $K_\|$. Dashed lines are $K_\| = 1$ where $\Omega_{\rm ii} = \Omega_{\rm cr}$ or $K_\|(K_{\perp,L=6.1} \to 0)$ where RH cutoff occurs at the inner boundary; (b) $\mathcal{A}$ as a function $\Omega_{\rm ii}$ and $\eta_{\rm He}$ converted from (a). The circles signify individual averaged wave frequencies detected by GOES-12 on 4:15, 4:20, 4:25, and 4:30UT from Figure 1. The crosses are the maximum and minimum frequency detected by GOES satellite ($\overline{\Omega}_{\rm obs}$) and helium concentration ratio ranges calculated in this letter. Using the average frequencies, the $\eta_{\rm He}$ can be inferred to 3.3, 3.4, 4.2, and 3.6 ± 0.7%, respectively. Here, the minimum density ratio can be estimated by assuming that the average frequency is the crossover frequency ($\overline{\Omega}_{\rm obs} \approx \Omega_{\rm cr}$).

The Princeton Plasma Physics Laboratory is operated
by Princeton University under contract
with the U.S. Department of Energy.

Information Services
Princeton Plasma Physics Laboratory
P.O. Box 451
Princeton, NJ 08543

Phone: 609-243-2245
Fax: 609-243-2751
e-mail: pppl_info@pppl.gov
Internet Address: http://www.pppl.gov